

Verification of the Back-EMF Method for Piston Velocity Measurements

R. Radebaugh, M. Lewis, and P. Bradley

National Institute of Standards and Technology
Boulder, CO 80305 USA

ABSTRACT

Linear compressors are used to drive pulse tube and Stirling cryocoolers, and they can be used as expanders in place of inertance tubes when inertance tubes cannot provide sufficient phase shifts between flow and pressure. Commercial linear compressors rarely incorporate position sensors, so PV power, flow rates, and flow-pressure phase at the piston are usually unknown. Use of the back EMF in linear motors to measure piston velocity was previously proposed. A comparison of this derived velocity with that determined from an accelerometer attached to the piston showed good qualitative agreement. However, no measurements have been reported on its accuracy or on comparisons with position sensors. We report here on a comparison of piston velocity measurements determined from the back-EMF method with those from a linear variable displacement transducer (LVDT) attached to a piston of a commercial linear compressor. Comparisons using a second compressor with a laser position sensor are also discussed. The back EMF is the complex voltage difference between normal operation and that where the pistons are locked to prevent movement for the same current. The velocity is simply the back EMF divided by the force constant of the motor. Measurements were made at 16 Hz, 30 Hz, and 60 Hz in both compressors. Our results show that the velocity amplitudes determined from the back-EMF method and the LVDT agree within 7 %. The laser position sensor showed abnormal behavior (20 % to 30 % deviations) for strokes less than about 20 % of full stroke. Agreement was within about 5 % at higher strokes. In terms of phase, the velocities from the laser sensor and the back EMF agreed within $\pm 2^\circ$ at 16 Hz and 30 Hz, but the velocity phase from the laser sensor lagged that of the back EMF by 13° at 60 Hz. The LVDT phase agreed within 2° with that of the back EMF at 16 Hz, but led as frequency increased. At 60 Hz the difference was 30° . Pressure measurements in a coupled reservoir also indicated the LVDT introduced a phase delay. We conclude that the back-EMF method has low uncertainty and can be used as a precision velocity sensor, as long as the compressor efficiency is greater than about 30 %.

INTRODUCTION

In the development of new regenerative cryocoolers, comparisons between experimental behavior and that predicted by models are of great importance. Of particular interest is a comparison of the input PV power, the volume flow rate at the piston face, and the phase between this flow and the pressure at the compressor (pressure oscillator). Such information is needed to fully characterize the pressure oscillator performance and the input conditions to the cold head. Due to cost considerations, position sensors are rarely incorporated into the commercial pressure oscillators

that are often used to drive new experimental cold heads. As a result, experimental information on the flow at the piston face is seldom obtained, which severely limits comparison with models. Because these pressure oscillators make use of DC magnetic fields and coils with AC currents that move relative to each other, an AC back electromotive force (EMF) is produced in the coils that is proportional to and in phase with the piston velocity. The back EMF reduces the current for a given applied voltage and results in a decreased motor force. The back EMF in rotary motors has been used extensively for motor control for many years. The maximum unloaded speed of a permanent magnet motor occurs when the back EMF, plus voltage associated with losses, equals the input voltage. Driving such motors turns them into generators because of this same back EMF, or voltage generated due to the relative motion of the coil and the magnetic field.

Redlich¹ first discussed the use of back EMF for the measurement and control of piston position in compressors with linear permanent magnet motors. The back EMF determines the velocity and the dynamic component of position, but Redlich showed that with additional measurements and the use of compressor parameters, such as the spring constant and the moving mass, the integration constant for the absolute position could be determined. However, for model comparisons, we are concerned only about the velocity, and to a lesser extent the dynamic part of the displacement and the acceleration. Doubrovsky, et al.² discussed the use of back EMF in linear compressors to determine piston velocity and acceleration, which they used for the reduction of vibration export in dual-opposed pistons in a master/slave arrangement. They compared the velocity determined from the back EMF with that determined with an accelerometer and found excellent agreement after making some adjustment of motor parameters. To our knowledge, there have not been direct comparisons of the back-EMF velocity measurements with those from position sensors. We report here on such measurements for two linear compressors, one with a linear variable displacement transducer (LVDT) and the other with a laser displacement transducer.

THEORY OF BACK EMF AND VELOCITY IN PERMANENT MAGNET MOTORS

The Lorentz force \mathbf{F} , which occurs when a current \mathbf{I} passes through a wire in a magnetic field \mathbf{B} , is given by

$$\mathbf{F} = \mathbf{I} \times \mathbf{B}l, \quad (1)$$

where l is the length of wire in the magnetic field. The bold variables indicate vector variables with magnitude and direction. The cross product in Eq. (1) indicates that the force is perpendicular to both current and magnetic field. The product Bl (with any $\sin\theta$ factor) is the force constant α of the linear motor, which is a parameter usually measured by compressor manufacturers. The magnitude of the force is given simply by

$$F = I\alpha, \quad (2)$$

The Faraday Law of Induction states that when a wire moves with velocity \mathbf{v} with respect to a magnetic field, an electromotive force (EMF) is induced in the wire, which is given by

$$\boldsymbol{\varepsilon} = \mathbf{v} \times \mathbf{B}l, \quad (3)$$

In a linear motor both a force and velocity occur, so the EMF given by Eq. (3) is then referred to as the back EMF, which opposes and reduces the current flow in the motor. The magnitude of this back EMF is then given by

$$\varepsilon_b = v\alpha, \quad (4)$$

where α is the same force constant used in Eq. (2). Thus the velocity magnitude and phase can be determined from a measurement of the force constant (a scalar quantity) and the back-EMF magnitude and phase. In reality, the force constant can be a weak function of piston position.

The total EMF across the motor with AC current flow is given by

$$\begin{aligned} \varepsilon_t &= \varepsilon_R + \varepsilon_L + \varepsilon_b \\ &= IR + j\omega LI + \alpha v, \end{aligned} \quad (5)$$

where R is the resistance, L is the inductance, ω is the angular frequency, and j is the imaginary unit. The resistive, inductive and back-EMF components are shown as phasor quantities in current \mathbf{I} and velocity \mathbf{v} . Figure 1 shows two examples of these EMF phasor components in the complex fre-

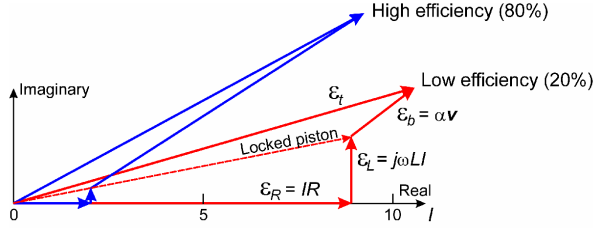


Figure 1. Phasor representation of EMFs associated with resistance, inductance, back EMF, and total EMF for the case of a low efficiency linear motor and a high efficiency linear motor.

quency domain. In the low efficiency case, the back-EMF magnitude is a small fraction of the total EMF magnitude. The example shown is for a compressor efficiency of about 20%. The other case is for a high compressor efficiency of about 80%. Accurate measurements of the back EMF in the low-efficiency case are difficult and require very accurate measurements of total voltage, current, resistance, and inductance. For the high-efficiency case, (more typical of a well designed system) uncertainties in current, resistance, and inductance are reduced by about a factor of five when propagated to the uncertainty of the back EMF. The measurement of R and L can be carried out by using an AC signal and measuring the real and imaginary components of the voltage, where current is along the real axis. The piston must be locked in such measurements to prevent any back-EMF contribution. When the piston is allowed to oscillate, the total voltage then contains the component due to the back EMF, ϵ_b . The real and imaginary parts of the voltage case may also contain components due to eddy currents and hysteresis. Locked and unlocked piston measurements should be made at the same frequency.

The relative magnitudes of ϵ_R and ϵ_b have a direct relationship to the compressor efficiency. The compressor efficiency is given by

$$\eta_{co} = \frac{\dot{W}_{PV}}{\dot{W}_{el}} = \frac{\dot{W}_m - \dot{W}_d}{\dot{W}_m + \frac{1}{2}|I|^2 R}, \quad (6)$$

where \dot{W}_{PV} is the PV power produced by the piston, \dot{W}_{el} is the electrical input power to the compressor, \dot{W}_m is the motor mechanical power, and \dot{W}_d is the damping power of the piston. The motor power can be expressed as

$$\dot{W}_m = \frac{1}{2} \pi \alpha |I| f s \sin \theta_m, \quad (7)$$

where f is the frequency, s is the peak-to-peak stroke, and θ_m is the phase between the current and the displacement. At resonance, the current and motor force are in phase with the velocity, so $\sin \theta_m = 1$ at resonance. The compressor efficiency for negligible damping is then given by

$$\eta_{co} = \frac{1}{1 + \frac{|I| R}{\pi \alpha f s \sin \theta_m}} = \frac{1}{1 + \frac{\epsilon_R}{\epsilon_b \sin \theta_m}}, \quad (8)$$

where the substitutions $\pi f s = v$ and $\epsilon_{Rb} = \alpha v$ were made in Eq. 8. We see from Eq. 8 that the ratio ϵ_R/ϵ_b is directly related to the compressor efficiency near resonance. For $\epsilon_R = \epsilon_b$, the compressor efficiency is 50% at resonance. Thus, for reasonably efficient compressors, the back EMF is large and easy to determine from the total EMF. In our measurements with no valve between the compressor and the reservoir, the power delivered is quite low, so $\sin \theta_m$ and h_{co} were quite small even near resonance (sharp resonance). Under normal operating conditions with a well-designed compressor driving a Stirling or pulse tube cold finger, $\sin \theta_m$ will usually be larger than about 0.7.

EXPERIMENTAL METHODS

Measurement Procedures

Figure 2 shows a schematic of the wiring and fluid connections for various electrical and compressor components. Voltage to the compressor is supplied by a signal generator and amplifier combination. The compressor current is determined by measuring the voltage drop across a

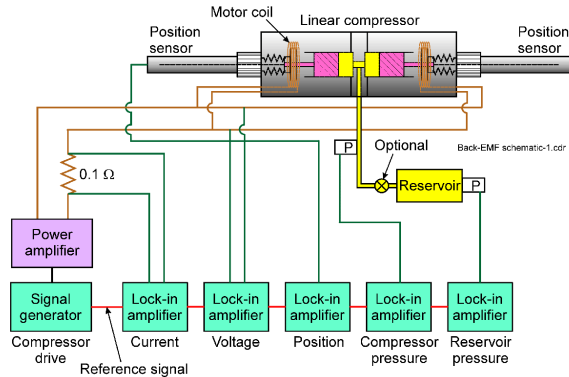


Figure 2. Schematic of fluid and electrical connections to a linear compressor for measurements reported here.

$0.102 \pm 0.001 \Omega$ resistor. Lock-in amplifiers are used to measure the amplitude and phase of voltage signals representing compressor current, compressor voltage, position, compressor pressure, and reservoir pressure, as shown in Fig. 2. The signal generator voltage is used as the reference signal for all lock-in amplifiers. A 50 cm^3 reservoir volume was coupled to the compressor output. The dynamic pressure in the reservoir is used to derive the mass flow at the reservoir entrance, which is nearly the same as the piston flow rate because the volume between piston face and reservoir entrance is only the piston swept volume and a void volume of about 2 cm^3 inside the compressor and the connecting tubing.

A needle valve can be used for the optional orifice indicated in Fig. 2. A valve was used in some preliminary measurements at low strokes for a self-consistency check on the force constant using the force balance on the compressor as shown by phasors for the heavily-loaded case in Fig. 3. This self-consistency check identified an error in the force constant that was being used for one of the compressors in our tests. We then measured the force constant for this compressor and found a reduction of about a factor of two compared with the manufacturer's value, presumably due to overheating of the NdFe magnet in some of our previous experiments. The sum of spring, gas, damping, and inertial forces then agreed with the motor force within about 5%. This self-consistency check requires the use of the optional valve in Fig. 2 in order to provide sufficient loading of the compressor. If the pressure amplitude is small (light load in Fig. 3), the motor force is small, which makes it difficult to determine the force constant accurately. The velocity comparison measurements were made without the valve in order to minimize the power dissipation and the necessity for an aftercooler. Pressure ratios of about 1.1 were experienced at full stroke, using the attached 50 cm^3 reservoir.

Test Compressors and Position Sensors

Characteristics of the two test compressors and their position sensors are listed in Table 1. The natural resonance frequency f_0 is the condition experienced by the compressor when the gas spring

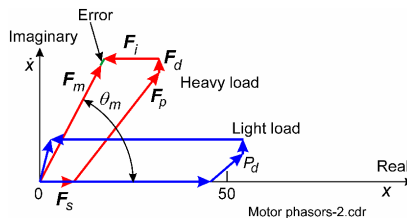


Figure 3. Phasor diagrams representing the force balance on a linear motor near resonance.

Table 1. Characteristics of two linear compressors used for velocity comparisons. The total swept volume V_{co} refers to the total of both sides, whereas maximum stroke s_{max} , force constant a , coil resistance R , inductance L , and maximum allowable current I_{max} refer to one side only. The natural frequency f_0 is the resonance frequency of the piston due only to the mechanical spring and moving mass (zero pressure amplitude). The force constant in parentheses for compressor #1 is our measured value after the compressor was accidentally overheated.

Compressor	Sensor	V_{co} (cm^3)	s_{max} (mm)	a (N/A)	R (Ω)	L (mH)	I_{max} (Arms)	f_0 (Hz)
#1	LVDT	4.3	10.0	17(8.87)	2.02	2.28	3.5	32.8
#2	laser	4.0	14.0	8.9	1.3	1.444	3.5	26.0

(pressure amplitude) is zero. For frequencies higher than f_0 , the spring force due to the pressure amplitude must be large enough to help offset the high inertial force if resonance is to be achieved. The linear variable displacement transducer (LVDT) on compressor #1 was calibrated in house. The LVDT sensitivity of the side used in our experiments was found to be 19.8 ± 0.1 mm/V when averaged over the entire 10 mm stroke. However, the sensitivity changed about ± 1.2 mm/V for the last 20 % of the full stroke. The sensitivity of the laser position sensor was set by the manufacturer to provide a sensitivity of 1.00 ± 0.01 mm/V. Figure 4 is a photograph of compressor #2 with its laser position sensor. A sapphire window on one of the back sides of compressor #2 allowed the beam from the external laser to reflect off the piston back side and impinge on the detector. The incoming beam was at a small angle with respect to the piston axis, so the intensity of the reflected beam at the detector varies with the piston position. The inductance of compressor #1 was not provided to us by the manufacturer, so we measured it using the same instruments and procedure discussed in the previous section. The only difference was that the pistons were locked using a threaded rod in place of the moving element of the position sensor. With the pistons locked there is no back EMF, and the total applied voltage is the phasor sum of only the resistive and inductive components. The real part (with respect to current) gives the resistive component and the imaginary part gives the inductive component. The frequencies and currents used covered the same range as the back-EMF measurements, but the resistance and inductance were independent of the frequency and current to within $\pm 1\%$. An LCR meter could have been used with the locked pistons, but the different instrument may have led to larger uncertainties.

Test Conditions

The frequencies and the corresponding average pressure used for the experiments were: 16 Hz, 0.1 MPa; 30 Hz, 0.8 MPa; 60 Hz, 2.5 MPa (compressor #1) and 2.0 MPa (compressor #2). The pressure ratio at full stroke was about 1.1. These pressures were chosen to keep the compressors operating close to resonance, to minimize the current for a given stroke. Measurements were made over a wide range of compressor voltages at each frequency. Figures 5 and 6 show how the ratio of resistive and inductive voltages to the back EMF varied with compressor voltage for the different operating conditions in the two compressors. The ratios are higher in compressor #1 because of its degraded force constant led to a smaller back EMF. Even in the worst case of 16 Hz and 60 Hz, the

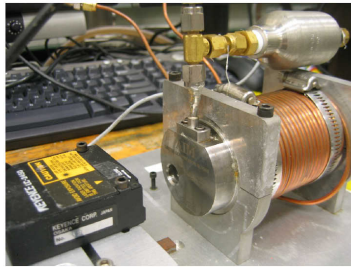


Figure 4. Compressor with laser position sensor.

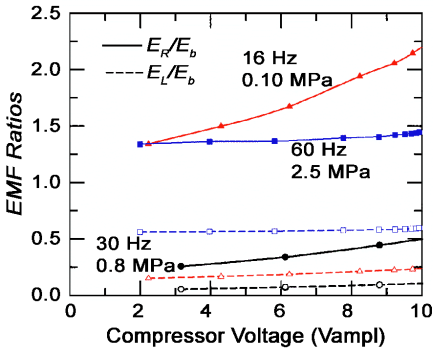


Figure 5. Ratio of resistive and inductive EMFs to the total EMF for compressor #1 for three frequencies.

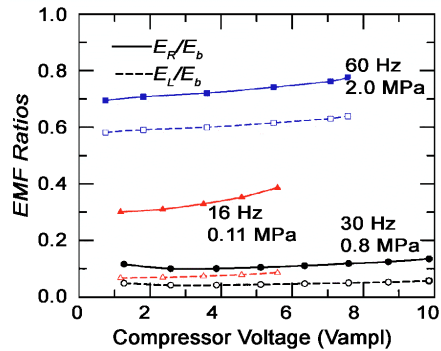


Figure 6. Ratio of resistive and inductive EMFs to the total EMF for compressor #2 for three frequencies

ratios are small enough to allow good measurements of the back EMF. A ratio of 2.0 simply means that a 1% error in resistance leads to a 2% error in back EMF and the associated velocity. In all of the measurements reported here, the resistance was measured several times during a measurement cycle using a four-lead DC ohmmeter to account for resistance changes as the coil heated. A 15 K temperature rise leads to a 5% change in the coil resistance, but a negligible change in inductance.

EXPERIMENTAL RESULTS

Displacement and Velocity Amplitudes

Figures 7 and 8 show the displacement amplitude in the two compressors as a function of motor voltage. In such a plot, the agreement between position sensors and back EMF appears to be good to within about 5 % of full stroke. Figures 9 and 10 show the fractional difference between the velocity amplitude v_{1Eb} determined from the back EMF and the velocity amplitude v_{1s} determined from the position sensor. Deviations are greatly magnified in such plots. Here we see that the back EMF and LVDT position sensor agree to within about 7% over the entire range. However, there is considerable disagreement between the back EMF and the laser position sensor at low voltages (strokes less than about 20 % of full scale). In order to determine which method is more reliable, we look at the mass flow rate at the reservoir entrance. This flow is given by

$$\dot{m}_r = \frac{\dot{P}V_r}{\gamma RT_r} \tag{9}$$

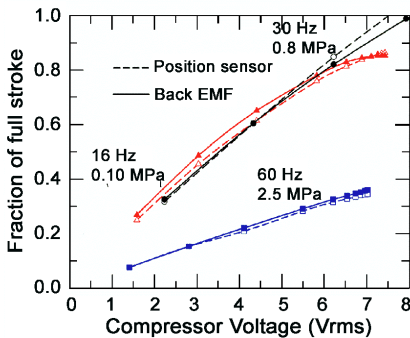


Figure 7. Comparison of displacement amplitudes for compressor #1 for three frequencies.

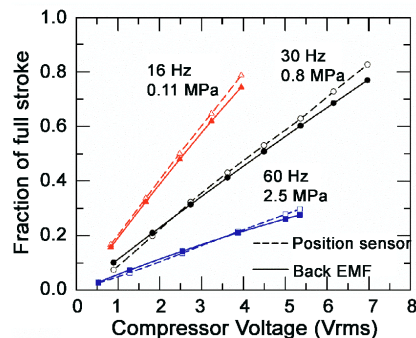


Figure 8. Comparison of displacement amplitudes for compressor #2 for three frequencies.

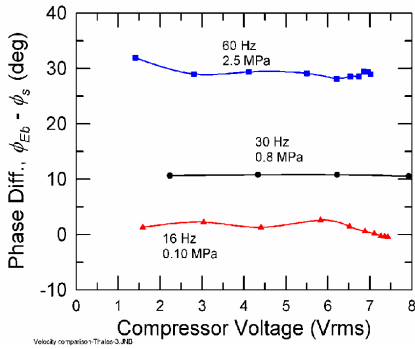


Figure 9. Fractional deviation of velocity amplitudes (back EMF – sensor) for compressor #1.

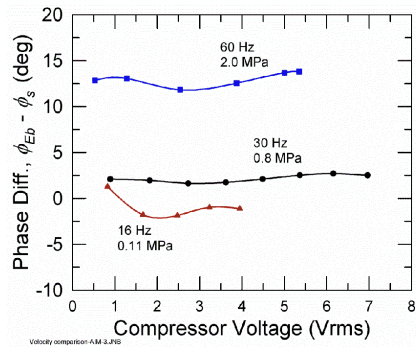


Figure 10. Fractional deviation of velocity amplitudes (back EMF – sensor) for compressor #2.

where \dot{p} is the time rate of change of the pressure in the reservoir, V_r is the reservoir volume, γ is the specific heat ratio, R is the gas constant for helium, and T_r is the reservoir temperature. Equation 9 assumes adiabatic processes in the reservoir. We expect flow at the piston face to be slightly higher (about 3% to 4%) due to the void volume in the compressor and connecting line to the reservoir. Figures 11 and 12 show the ratio of piston flow rate to reservoir flow rate for the two compressors. The high ratio at 60 Hz for compressor #1 is most likely due to piston blowby at this high pressure of 2.5 MPa. Other measurements at 1 MPa and 60 Hz were made, which gave a ratio of about 1.18, indicating less blowby at the lower pressure. Of particular interest are the curves in Figure 12, which show that the piston flow due to the laser position sensor drops much below the reservoir flow at low compressor voltages for 30 Hz and 60 Hz. The piston flow due to the back EMF velocity is in much better agreement with the reservoir flow. We then conclude that the laser position sensor is in error at low strokes, and that the back EMF gives more accurate results for the velocity amplitude over the whole range of strokes.

Velocity Phase

Figures 13 and 14 show the velocity phase difference between that due to the back EMF, ϕ_{Eb} , and that due to the position sensor, ϕ_s . We note in Fig. 13 that ϕ_{Eb} leads ϕ_s more as the frequency increases, as if the LVDT is too slow. The laser sensor and the back EMF are in much better agreement, as shown in Fig. 14. To help determine which phase is correct, we make use of Eq. 9, which shows that \dot{m}_r should be in phase with \dot{p} . The additional flow at the piston face due to the

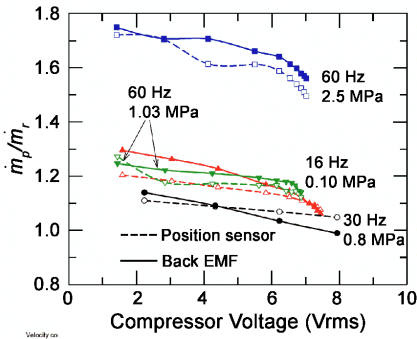


Figure 11. Ratio of piston flow rate to reservoir flow rate with compressor #1.

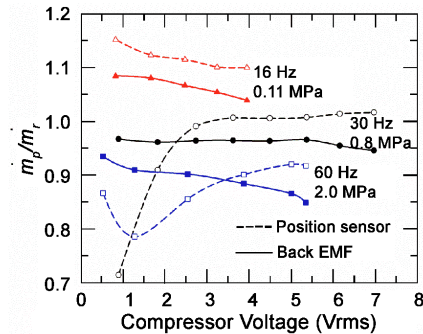


Figure 12. Ratio of piston flow rate to reservoir flow rate with compressor #2.

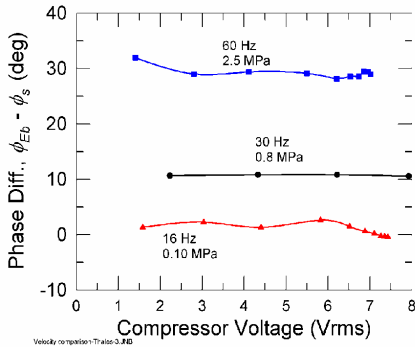


Figure 13. Phase difference between back EMF and sensor velocities for compressor #1.

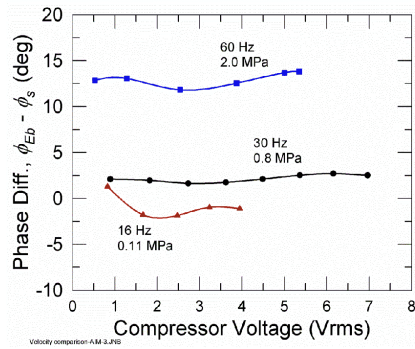


Figure 14. Phase difference between back EMF and sensor velocities for compressor #2.

small void volume in the compressor and transfer line is also in phase with \dot{p} . Therefore, the void volume will not affect the velocity phase. However, the use of flow impedance before the reservoir would cause the piston flow to lead the reservoir flow in the presence of void volume before any impedance. The distance between the piston face and the pressure transducer in the reservoir is about 30 cm. The acoustic wavelength in helium at 60 Hz is about 20 m. Thus, the pressure wave is delayed by about $0.3 \times 360 / 20 = 5^\circ$ between the piston and reservoir transducer.

Figures 15 and 16 show the phase difference between the piston velocity and the reservoir \dot{p} . The large phase lags of the LVDT position sensor, shown in Fig. 15 clearly indicate the LVDT is too slow for frequencies above 16 Hz, whereas the back EMF phase shows no sign of any significant delay. The small delay of about 10° may be due to a small, but finite, amount of heat transfer between the gas and the tube walls, which causes a slight delay in the piston flow. This delay decreases at higher frequencies, as indicated by the back EMF curves in Fig. 15. The phase differences associated with the laser position sensor, shown in Fig. 16, are much smaller and agree well with those of the back EMF, except for 60 Hz. The pressure phase delay (flow leading) of 7° to 13° in Fig. 16 for 60 Hz is only slightly larger than the 5° phase shift expected at 60 Hz because of the acoustic wavelength effect discussed earlier.

CONCLUSIONS

The back EMF in linear permanent-magnet motors is a direct effect of the fundamental Faraday law of induction in a wire moving with respect to a static magnetic field. This back EMF is

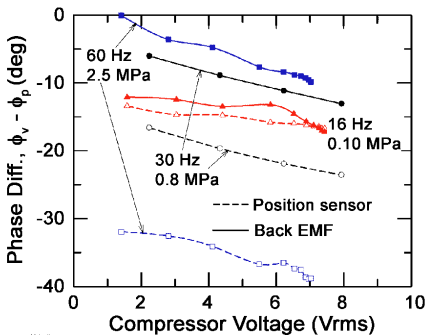


Figure 15. Phase difference between piston velocity and pressure time derivative for compressor #1.

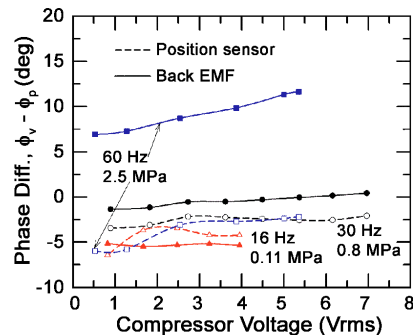


Figure 16. Phase difference between piston velocity and pressure time derivative for compressor #2

exactly equal to the motor force constant times the velocity. Because the force constant is usually measured by linear compressor manufacturers, measurement of the back EMF amplitude and phase can be used to determine the flow amplitude and phase at the piston face, without the need for an explicit position sensor. The EMF associated with the coil resistance and inductance must be subtracted (real and imaginary parts) from the total motor EMF to find the back EMF. The uncertainty of the back EMF is mostly associated with the uncertainties of the resistance and inductance. The resistive and inductive EMFs are generally less than the back EMF for motor efficiencies greater than about 50 %. We compared the amplitude and phase of velocity determined from the back EMF in two commercial compressors with those determined by position sensors attached to the compressors. One compressor had a linear variable displacement transducer (LVDT) attached and the other used a laser position sensor. Frequencies of 16 Hz, 30 Hz, and 60 Hz were used in the comparisons. Measurements were made with the compressors connected to a reservoir of known volume with an attached pressure transducer, which provided an independent check on the flow rate. Our results showed that the piston velocity determined from the back EMF was more accurate than the velocity measured by either of the position sensors. We estimate the uncertainties associated with our measurements of the back-EMF velocity to be less than about 5 % in amplitude and less than about 5° in phase. The velocity determined from the LVDT position sensor agreed with that of the back EMF within about 10 % in amplitude, but showed a phase lag of about 30° at 60 Hz. The velocity from the laser position sensor agreed within 10 % in amplitude at large strokes but under predicted the velocity by 20 % to 30 % at small strokes. Its phase agreed with that of the back EMF to within about 10°. We conclude that the back-EMF method provides a very accurate measurement of the piston velocity in linear compressors.

ACKNOWLEDGMENT

This research was partially funded by the Office of Naval Research with Deborah Van Vechten as the project monitor.

REFERENCES

1. Redlich, R. W., "Method and apparatus for measuring piston position in a free piston compressor," U.S. Patent 5,342,176 (1994).
2. Doubrovsky, V., Veprik, A., and Pundak, N., "Sensorless Balancing of a Dual-Piston Linear Compressor of a Stirling Cryogenic Cooler," *Cryocoolers 13*, Kluwer Academic/Plenum Publishers, New York (2005), pp. 231-240.

